Sand deformation under proportional loading

D. NEGUSSEY AND Y. P. VAID
Department of Civil Engineering, The University of British Columbia, Vancouver, B.C., Canada V6T 1W5

Received July 29, 1985
Accepted January 20, 1986

A fundamental experimental study of sand behaviour under low stress ratio proportional loading wherein all strain components are contractant is presented. Experimentally observed behaviour under stress conditions of the triaxial test led to a coherent framework for representing proportional loading stress–strain response. The stress–strain relationship formulated incorporates relative density as an inherent independent state variable and does not require appeal to material isotropy.

Key words: triaxial test, proportional loading, sand, relative density, energy density, stress increment, strain increment.

L'on présente une étude expérimentale fondamentale sur le comportement du sable sous chargement proportionnel à faible rapport de contraintes où toutes les composantes de déformation sont en compression. Le comportement expérimental observé dans les conditions de contrainte de l'essai triaxial amène à un cadre cohérent pour la représentation de la réaction au chargement proportiononel contrainte–déformation. La relation contrainte–déformation formulée incorpore la densité relative comme variable d'un état inhérent indépendant et ne requiert pas de faire appel à l'isotropie du matériau.

Mots clés: essais triaxiaux, chargement proportionnel, sable, densité relative, densité d'énergie, incrément de contrainte, incrément de déformation.

Can. Geotech. J. **23**, 155–163 (1986)

[Traduit par la revue]

Introduction

Accurate material characterization is a necessary prerequisite for a satisfactory solution of deformation problems of soil masses using numerical techniques. Various material models, such as incremental elastic, elastoplastic, and particulate, have been used to represent the stress–strain response of sand. Such representations have in general concentrated on modelling of behaviour in the domain of large strains (generally in excess of 10^{-3}). To the writers' knowledge, no direct assessment has been made of the capability of these models in representing small strain (between 10^{-5} and 10^{-2}) response. In many situations, working stresses under drained conditions induce strains that are less than 10^{-2}. Similarly, the development of positive pore presure during undrained loading is a phenomenon that occurs mainly at small strains.

Incremental elastic representation of sand using hyperbolic approximations is recognized to be not valid in the region of small strains (Duncan and Chang 1970). Evidence presented in support of elastoplastic representation of sand behaviour (Poorooshasb *et al.* 1966) does not hold at small strains (Negussey 1984) with respect to the unique association of strain increment direction to the state of stress. Similarly, particulate representation, such as by stress dilatancy, is not possible in the region of small strains, wherein all strain components are often compressive and, thus, the energy increment ratio is not negative, as required in the theory (Rowe 1962).

Since behaviour of soils is stress path dependent, any new approach of small strain response will be better pursued by a study of behaviour under simple stress paths. Proportional loading paths are of fundamental importance in the study of deformation response of metals and other solids (Mehan 1961; Rees 1981). Sand is a frictional material for which strain response and failure are strongly dependent on effective stress ratio. Proportional loading paths are therefore of even more fundamental importance in the study of deformation response of sand. During such loading paths, stress components increase proportional to each other and thus the overall obliquity of applied stresses remains fixed. Below a threshold obliquity of applied external loads, proportional loading in sand induces stiffening. Furthermore, as long as the overall obliquity remains well below that corresponding to the material sliding friction, no tendency for major interparticle slip would exist. The associated internal change of geometry would then likely result in net contraction, and corresponding strains will be small.

Proportional loading resonse of loose and dense sand has been investigated by Barden *et al.* (1969), El-Sohby (1969), El-Sohby and Andrawes (1972), and Rowe (1971). These studies examined general characteristics of loading and unloading response of either loose or dense sand with a view towards an elastic–plastic idealization of behaviour. Quantitative relationships across relative densities have, in general, not been successful. More importantly, the implicity but key assumption regarding the elastic character of recovered deformations and the possible separation of elastic and plastic strains still remains in doubt (Coon and Evns 1969; Zytynski *et al.* 1978). Attempts to describe the observed behaviour by stress-dilatancy theory were also unsuccessful (Barden *et al.* 1969; Rowe 1971). This lack of agreement with theory persisted even after attempted separation of strains into elastic and slip components by a load–unload process, and consideration of only presumed slip components (Barden *et al.* 1969). In the region of low stress ratios the strain response is entirely contractant (when all strain components are compressive). Stress dilatancy then is not applicable in principle, since the energy increment ratio is not negative, as required in the theory (Rowe 1962).

The investigations presented in this paper constitute a study of the fundamental behaviour of sand under low stress ratio proportional loading and the associated small strains. This study examines total strain response to constant R (principal effective stress ratio) axisymmetric loading and forms part of a broader investigation of small strain response of sand. Quantitative relationships between stress and strain for constant R paths leading to contractant strain response are explored and a stress–strain relationship, which incorporates relative density of sand as a state variable, is formulated.

Experimental

A uniform, clean quartz sand, Ottawa sand ASTM-C-109, was used in all tests. Ottawa sand has subrounded to rounded particles with $D_{50} = 0.4$ mm and $C_u = 1.5$. Maximum and minimum void ratios determined by the test method ASTM D2049 are 0.82 and 0.50, respectively.

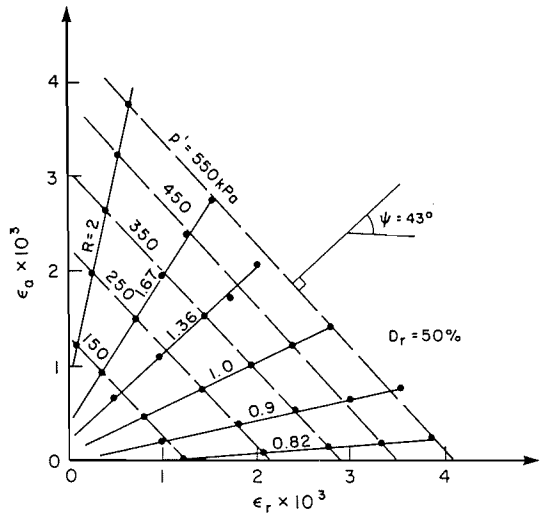

FIG. 1. Proportional loading strain paths and p' equipotentials.

A pneumatic stress path analog (Vaid and Negussey 1983) was employed to pursue proportional loading stress paths in the 'triaxial' stress plane. A critical evaluation of available procedures for assessment of volume change due to membrane penentration was made, and improved methods were developed and adopted (Vaid and Negussey 1984). Smooth anodized aluminum end plattens with centrally located 20 mm diameter porous stones were used to diminish bedding errors and end restraint. Because of the associated large bedding errors (Sarsby *et al.* 1980) and their marginal usefulness for small strain considerations (Barden *et al.* 1969; Rowe and Barden 1964), lubricated end plattens were not used in this investigation. Test specimens were of 63.5 mm diameter and height-to-diameter ratio of 2:1. Use of this sample geometry and a careful minimization of apparatus compliance permitted accurate measurement of small deformation with sensitivities of the order of 10^{-5} in both axial and volumetric strain measurements.

Sand samples were prepared within a cavity formed by the rubber membrane that lined the split mold and by pluviation through water. No densification was done during pluviation and thus all samples were loose and had the same relative density at the termination of the deposition process. Desired relative densities were then obtained from the known dry weight of sand used and controlling specimen heights.

After it was connected to the volume change and pore pressure measuring device, the test sample was brought to an effective hydrostatic stress state of 50 kPa with a back pressure of 100 kPa. In order to bring the stress state of the specimen to the desired stress ratio R, a deviator stress was then applied under drained conditions, with the effective confining pressure held constant. This stress state was taken as the initial stress state for the test.

Test results

Behaviour of medium dense specimens

Results of several constant R path tests on specimens of Ottawa sand at a relative density of 50% are shown in Fig. 1. The stress ratio, R, is expressed as the ratio of axial, σ_a', to radial, σ_r', stress. Tests that have $R > 1$ are in states of compressional deviatoric stress ($\sigma_a > \sigma_r$). The test for which $R = 1$ corresponds to hydrostatic loading ($\sigma_a = \sigma_r$) and stress paths with $R < 1$ are in extensional deviatoric stress state ($\sigma_a < \sigma_r$). Overall stress ratios in the tests range between 0.82 and 2.

The results have been presented in the 'triaxial' strain plane (ϵ_a vs. $\sqrt{2}\epsilon_r$). It may be noted that constant R stress paths result in linear strain paths in strain space. Such linear strain paths during constant R loading have also been observed by others (Barden *et al.* 1969; El-Sohby 1969, El-Sohby and Andrawes 1972; Rowe 1971). Since the strain paths are linear, the incremental strain ratios are constant and equal to the total strain ratio for a given stress path. All of the strain paths have positive slopes and are contained within the first quadrant of strain space. Thus both axial and radial strain increments are contractant, whether the mode of loading is compressional or extensional.

Along the positive axial strain axis, radial strains are zero. This strain path of zero lateral deformation is associated with a stress path that is commonly known as the K_0 path. Axial strains are zero along the positive radial strain axis. A strain path oriented at an angle of 35° to the horizontal represents a path of equal axial and radial strain increments. In Fig. 1 the observed strain path for hydrostatic compression ($R = 1$) does not coincide with this 35° line. Deformation under hydrostatic loading is such that the radial strains are greater than the axial strains. The specimen thus possesses an inherent anisotropy, as has been observed (Arthur and Menzies 1972; El-Sohby and Andrawes 1972; Oda 1972; Yamada and Ishihara 1979). The linearity of strain paths also implies that anisotropy is fixed by R and is not altered by increasing mean effective stress along the R paths (Rowe 1962).

It is of interest to point out here that biaxial, constant R loading of metals in the plastic range has also been shown to result in linear plastic strain paths (Mehan 1961; Rees 1981). Linearity of strain paths would imply that the material response can be described by the deformation theory of plasticity and that the nature of inherent anisotropy is not altered by stress-induced anisotropy (Rees 1981).

Soils differ from metals (which are incompressible during plastic deformation) because of their irreversible, dilatant as well as contractant response to loading. Load increase even at small stress ratios may lead to creep and fracture in metals, whereas below a threshold obliquity of applied external loads, proportional loading in soils induces stiffening in the range of stresses normally encountered. These differences in behaviour are fundamental in distinguishing these broad material classifications.

The strain increment ratio, defined as the ratio of axial strain increment to $\sqrt{2}\times$ radial strain increment, $\epsilon_a/\sqrt{2}\epsilon_r$, would be zero for horizontal strain paths. This ratio would tend to infinity for paths approaching the vertical. If these strain ratios were expressed as tangent inverses, the ensuring angle, θ, will range from 0 to 90°. Such angles of strain increment ratios in the triaxial strain space of Fig. 1 are plotted against corresponding stress ratios in Fig. 2. A linear relationship may be noted that is valid in regions of both compression and extension. Continuity of the relationship across compression and extension is maintained by expressing extensional stress ratios as negative inverses of those in compression. Similar representation of stress ratio has been adopted in the study of metal behaviour under proportional loading (Mehan 1961; Rees 1981). Since there is a discontinuity in the stress ratio axis at $R = 1$, separate expressions relating strain increment ratio to stress ratio must be used in the extension and compression sides. But since the slope is the same and $R = 1$ is common to both compression and extension, either relationships can be derived from the other. Thus, strain increment ratios for compressional paths may be expressed by

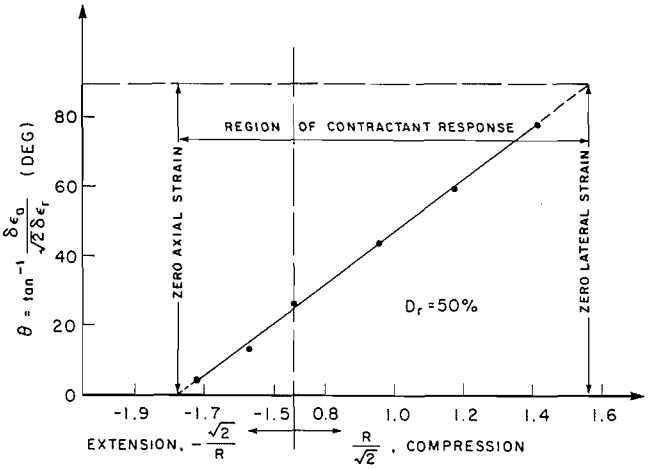

FIG. 2. Relationship between strain increment ratio and stress ratio.

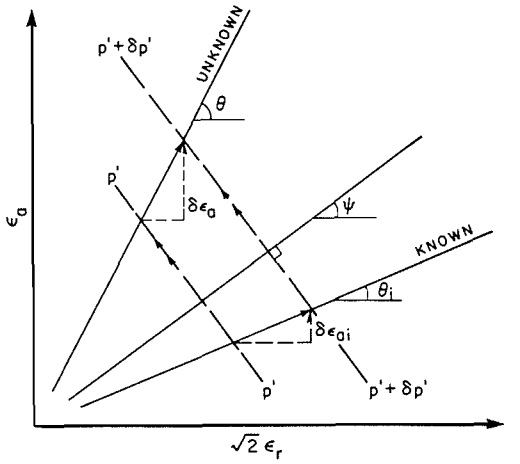

FIG. 3. Geometric features of strain paths and p' equipotentials.

$$[1] \quad \frac{\delta\epsilon_a}{\sqrt{2}\delta\epsilon_r} = \tan\left[a + b\left(\frac{R}{\sqrt{2}}\right)\right]$$

and for extensional paths

$$[2] \quad \frac{\delta\epsilon_a}{\sqrt{2}\delta\epsilon_r} = \tan\left[c + b\left(\frac{-\sqrt{2}}{R}\right)\right]$$

For the result on Ottawa sand shown in Fig. 2, $a = -28$, $b = 75$, and $c = 134$.

Since for $R = 1$, [1] and [2] should yield identical values of strain increment ratio, $(a + b/\sqrt{2}) = (c - \sqrt{2}b)$, which means that only two of the three constants a, b, and c are independent.

In Fig. 1, if points representing equal mean normal effective stress $p' = \frac{1}{3}(\sigma_a' + 2\sigma_r')$ along the linear strain paths are connected, the resulting locus is a straight line. Such straight-line loci may be seen to be parallel for different values of p'. These straight lines will be referred to subsequently as equipotentials of p'. The gradient of equipotentials of p', i.e. the strain path that is normal to equipotentials of p', has a slope $\psi = 43°$ for the sand tested. From Fig. 2 it may be seen that such a strain path will result for a stress path with $R = 1.30$.

Stress–strain relationship at one relative density

The deformation behaviour observed so far can be structured to form a simple proportional loading stress–strain relationship that is valid for constant R paths in the first quandrant of strain space. The foundations of this relationship lie in the observed linearity and parallel orientation of equipotentials of effective mean normal stress and the linear relationship between stress ratio and θ. Thus, the strains along a desired R path could be predicted using the stress–strain relationship for a known R path.

Essential features of Fig. 1 are represented in a simplified form in Fig. 3. Values θ_i and θ are tangent inverses of strain increment ratios along the known and arbitrary R paths, respectively, whereas ψ is associated with strain increment ratios along the strain path coincident with the gradient of p'. Consider the known and arbitrary R paths at points of identical mean normal stress p' and the sand subjected to equal increments of mean normal stress $\delta p'$. Let the resulting axial strain increment for the known stress paths be $\delta\epsilon_{a_i}$. Then, from geometrical considerations, the corresponding strain increment, $\delta\epsilon_a$, along the desired R paths may be shown to be

$$[3] \quad \delta\epsilon_a = \frac{\sin\theta}{\sin\theta_i}\frac{\cos(\theta_i - \psi)}{\cos(\theta - \psi)}\delta\epsilon_{a_i}$$

Since the volumetric strain increment

$$[4] \quad \delta\epsilon_v = \delta\epsilon_a + 2\delta\epsilon_r$$

and noting that

$$[5] \quad \frac{\delta\epsilon_a}{\sqrt{2}\delta\epsilon_r} = \tan\theta$$

the volumetric strain increments for the desired R path become

$$[6] \quad \delta\epsilon_v = \left(1 + \frac{\sqrt{2}}{\tan\theta}\right)\delta\epsilon_a$$

Equations [3] and [6] together with the relationships [1] and [2] have been used to develop the stress–strain predictions shown in Fig. 4. The known data base for these prediction was the hydrostatic compression ($R = 1$) test. Stress–strain predictions for both compressional and extensional constant R paths have been made and compared with the observed stress–strain results. Even though the strains are very small, excellent agreement may be noted between the observed and predicted stress–strain response for both compressional and extensional modes.

The proportional loading stress–strain behaviour of sand at one relative density is therefore completely specified if results of two tests at different R values are known. One of such tests can be the simple hydrostatic compression ($R = 1$) test. The second test could be carried out at any other value of R, compressional or extensional. The results of these two tests will enable determination of all constants, namely a, b, c, and ψ, needed for a complete specification of proportional loading behaviour. The stress–strain results of any one of the two tests can serve as the reference data base for strain predictions under any R path loading.

The relationship expressed by [3] has been derived from experimental results. This relationship has an important implication regarding the ratio of energy density increment (incremental energy input per unit volume) between any two constant R paths. The increment in energy density δE resulting from an increment in stress is

$$[7] \quad \delta E = \sigma_a'\delta\epsilon_a + 2\sigma_r'\delta\epsilon_r$$

If the stress increment is along a constant R path for which

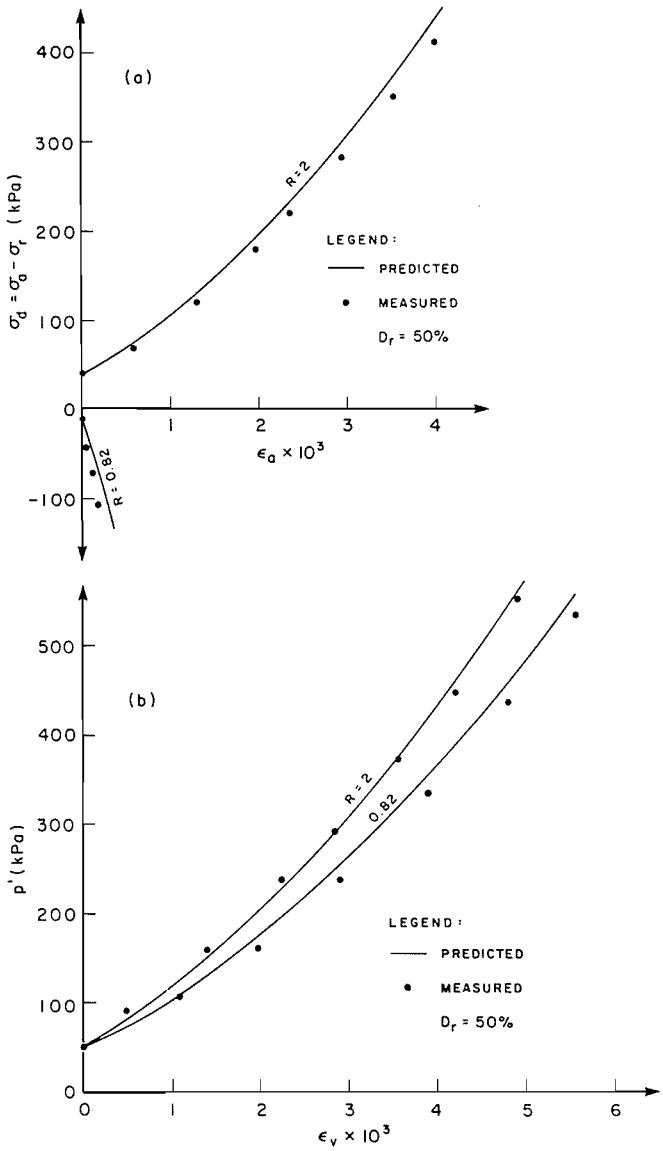

FIG. 4. Comparison of measured and predicted strains: (*a*) axial strain; (*b*) volumetric strain.

$\sigma_a'/\sigma_r' = R$, $\sigma_r' = 3p'/(R+2)$, and $2\delta\epsilon_r/\delta\epsilon_a = \sqrt{2}/\tan\theta$, [7] can be written as

$$[8] \quad \delta E_R = \left[\frac{3}{R+2}\left(R + \frac{\sqrt{2}}{\tan\theta}\right)\right] p' \delta\epsilon_a$$

in which the subscript on E refers to stress increment along a constant R path. For a given R path, $\tan\theta$ is constant. Therefore, the expression in square brackets in [8] is a constant along the entire stress path. The energy density increment ratio of any two stress paths at identical values of p' would thus be proportional to the ratio of their axial strain increments. This ratio of axial strain increments may be seen to be a function of θ values associated with the two stress paths and the angle ψ ([3]). Since both θ values are fixed for the specified stress paths and ψ is constant, the ratio of the axial strain increments is constant along the entire stress paths. Hence the energy density increment ratio of the two R paths with identical mean normal stress histories is also constant.

The ratios of energy density increment at various R values to the energy density increment at reference hydrostatic stress ratio

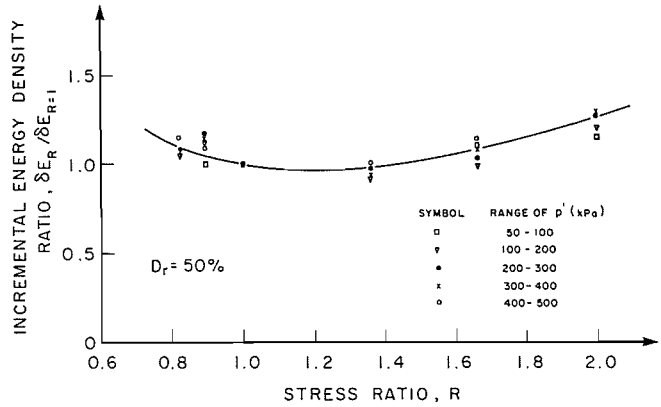

FIG. 5. Variation of incremental energy density ratio with stress ratio.

$R = 1.0$ are shown in Fig. 5. It may be seen that for each R, this ratio is essentially constant, regardless of the level of p' and attains a minimum for $R \sim 1.20$, which corresponds approximately to a stress ratio yielding an isotropic strain condition (see Fig. 2). Thus, the minimum energy density state appears to be associated with a stress ratio giving rise to a state of isotropic strain.

Extensions to other relative densities

The previous observations and stress–strain predictions were based on results obtained from tests on sand at a relative density of 50%. Additional tests were made to investigate possible extensions to the behaviour at other relative densities. Two series of tests, one each on loose and dense specimens at relative densities of 30 and 70%, were carried out.

Test results on loose and dense specimens in the form of Fig. 1 are presented in Fig. 6. Once again, constant R stress paths may be seen to result in linear strain paths for both relative densities. Also, equipotentials of mean normal stress seem linear and parallel with essentially the same orientation for all relative densities. This implies that ψ is independent of relative density. As would be expected, for equal stress states the magnitude of contractant strain response decreased markedly with increase in relative density.

Results of tests on specimens of different relative densities but at equal stress ratios are presented in Fig. 7. Under hydrostatic loading at $R = 1$ the slope θ of the strain path for the dense sample is ~35°, which implies isotropic behaviour. With decreasing relative density, inherent anisotropy increases progressively as the slope of the strain path deviates more and more below 35°. It may also be noted that equipotentials of mean normal stress connecting strain paths of equal R but different relative densities are essentially linear and parallel. The gradient of these p' equipotentials, however, is not constant but depends upon the value of R.

Relationships between stress raio, R, and strain increment ratios at different relative densities are shown in Fig. 8. As observed previously for relative density of 50%, linear relationships between stress ratio and θ, the tangent inverse of the strain increment ratio, may also be noted for other relative densities. The slope of these relationships, however, decreases as the relative density increases. The existence of increasing inherent anisotropy with decreasing relative density is again indicated by the data points (deviation of θ from 35°) corresponding to the hydrostatic, $R = 1$ loading.

The relationships between θ and relative density at several

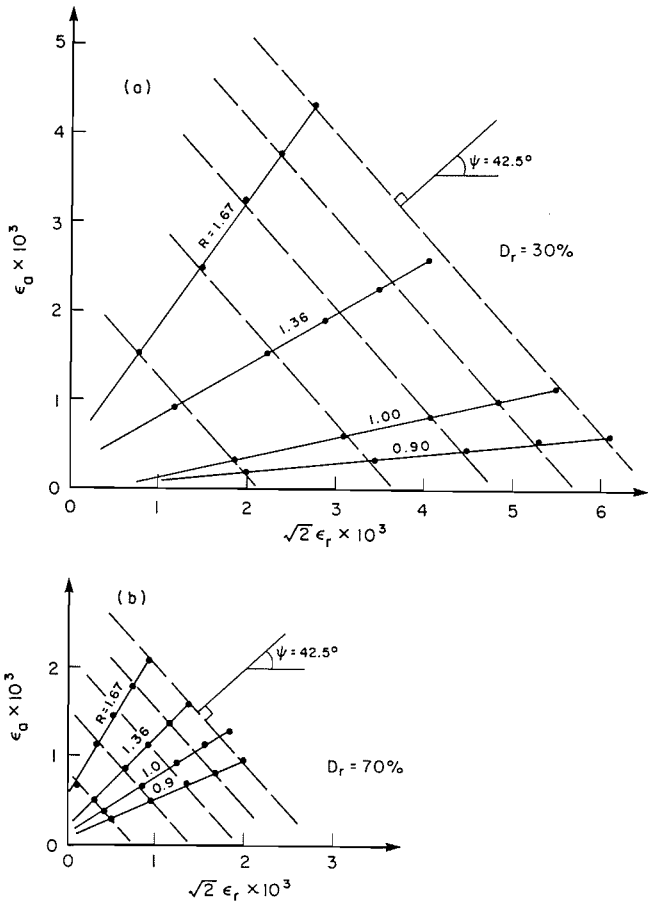

FIG. 6. Proportional loading strain paths and p' equipotentials: (a) $D_r = 30\%$; (b) $D_r = 70\%$.

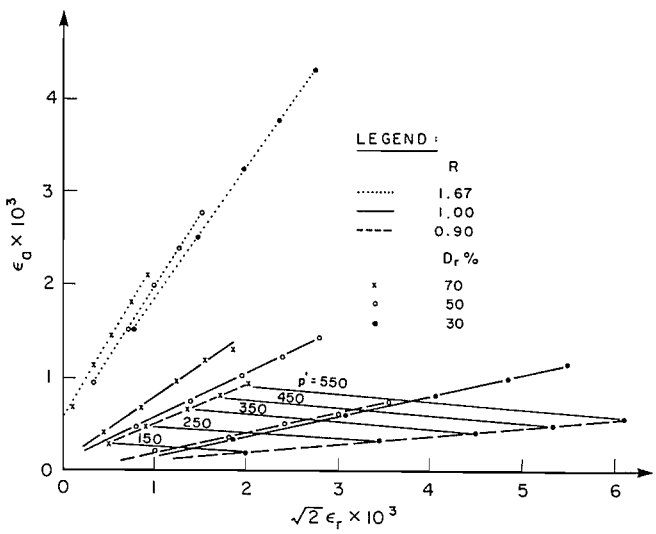

FIG. 7. Strain paths for proportional loading at various relative densities.

constant values of R are shown in Fig. 9. It may be noted that linear relationships exist between θ and relative density at each value of R. The slope of these straight lines decreases progressively with increasing R.

The linear relationships observed in Figs. 8 and 9 when combined result in a plane surface in three dimensions with % relative density D_r, stress ratio R, and θ as coordinates. The equation of this plane, which describes the contractant proportional loading behaviour of sand, is, for compression,

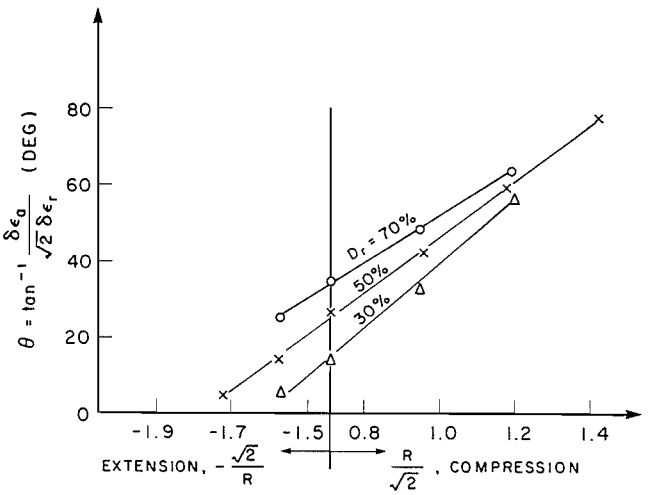

FIG. 8. Relationships between strain increment ratio and stress ratio at different relative densities.

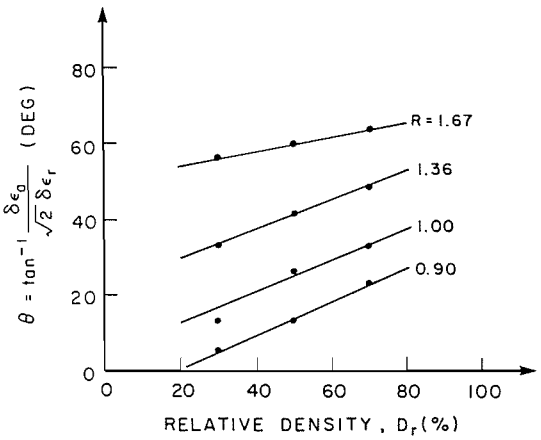

FIG. 9. Relationships between strain increment ratio and relative density for different stress ratios.

$$[9] \quad D_r + A\left(\frac{R}{\sqrt{2}}\right) + B\theta + C = 0$$

and for extension,

$$[10] \quad D_r + A\left(\frac{-\sqrt{2}}{R}\right) + B\theta + D = 0$$

in which A, B, C, and D are constants. Since $R = 1$ is common to compression and extension, this requires $(A/\sqrt{2} + C) = (-\sqrt{2}A + D)$, and thus there are only three independent constants. For Ottawa sand the values of the constants are $A = 189$, $B = -2.6$, $C = -115$, and $D = 287$ and the plane surface represented by [9] and [10] for this sand is shown in Fig. 10. Required constants for the equation of this plane surface can be determined by performing three proportional loading tests.

Magnitudes of the strain increment ratio under proportional loadings can therefore be specified for arbitrary R and D_r, once the plane surface as in Fig. 10 has been established for the sand. This unique relationship of strain increment ratio to stress ratio R and relative density is in principle similar to the stress-dilatancy theory (Rowe 1962). The stress-dilatancy theory, however, neither enables precise numeric prediction of the strain increment ratio (only provides upper and lower bounds)

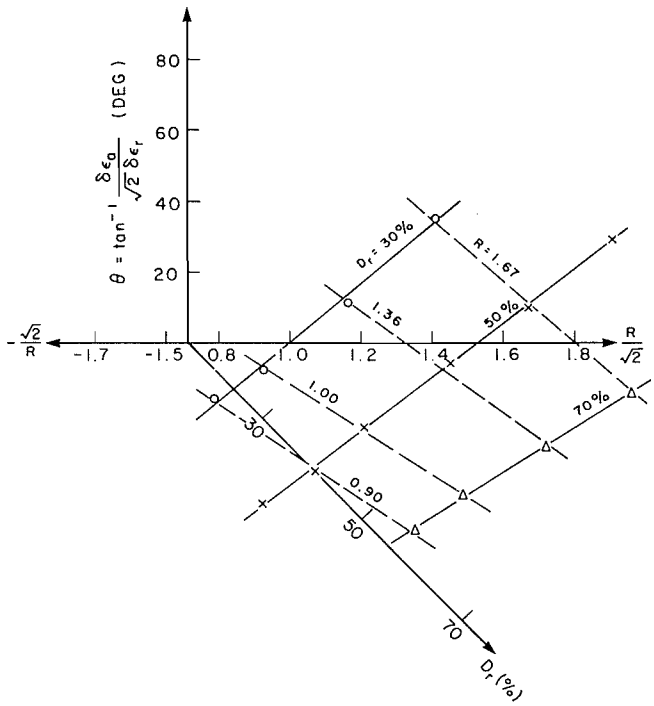

FIG. 10. Contractant constant R state surface for Ottawa sand.

nor takes explicit account of the relative density as a state variable. Furthermore, the stress-dilatancy theory cannot, in principle, describe contractant deformation response of sand, in which there is no rate of energy out in either principal directions.

The ability to predict strain increment ratio alone for any R value does not, however, enable determination of individual strain components. The determination of these individual strain components will now be attempted by establishing energy density increment relationships across relative densities, similar to those discussed earlier at one relative density.

From the examination of test results at one relative density of 50%, it has been shown that the ratio of axial strain increments of two R paths are constant provided the mean normal stress histories are identical. The implications of that result was demonstrated to require the ratio of energy density increments to be constant all along the two stress paths (Fig. 6). A similar behaviour with regard to constancy of energy density increment ratio may be seen in Fig. 11 for relative densities of 30 and 70%. It would now be of interest to examine possible energy density increment ratio relationships between specimens having identical stress histories (p' and R) but different relative densities. Such energy density increment ratios are shown plotted against stress ratio R in Fig. 12. At each relative density, the energy density increment ratio shown is the ratio with respect to the energy density increment for $D_r = 50\%$. The results in Fig. 12 suggest that for any value of R the energy density increment ratio of two specimens having identical stress histories but different relative densities remains reasonably constant. Furthermore, the magnitude of this ratio is essentially the same regardless of the identical R value for which the energy density increments are considered. Average lines have been drawn in Fig. 12 through data points for each energy increment ratio considered, in order to determine the constant values of these ratios.

Values of the constant energy density ratios in Fig. 12 are now plotted against the inverse ratio of the corresponding

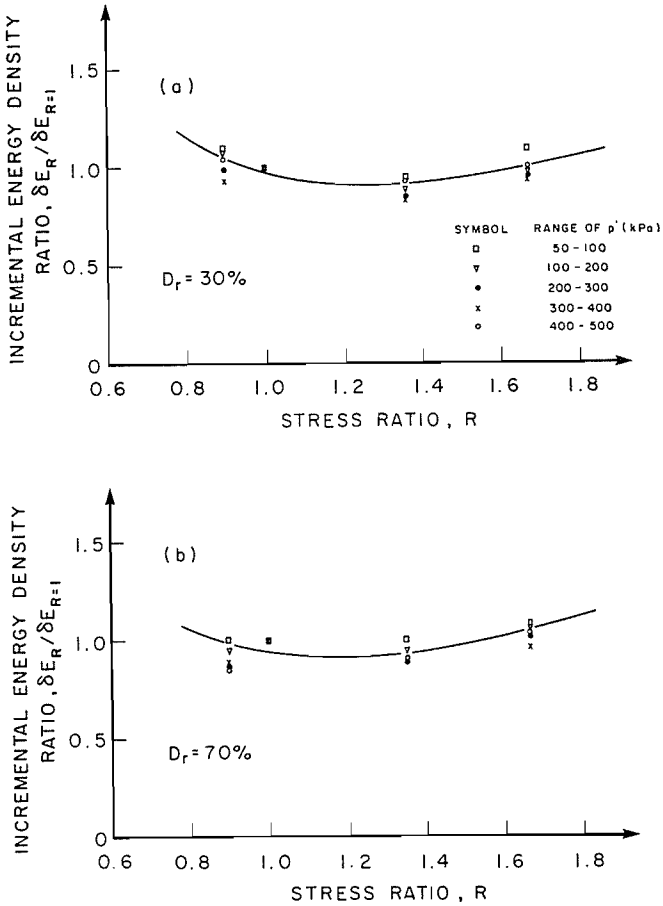

FIG. 11. Variation of incremental energy density ratio with stress ratio: (*a*) $D_r = 30\%$; (*b*) $D_r = 70\%$.

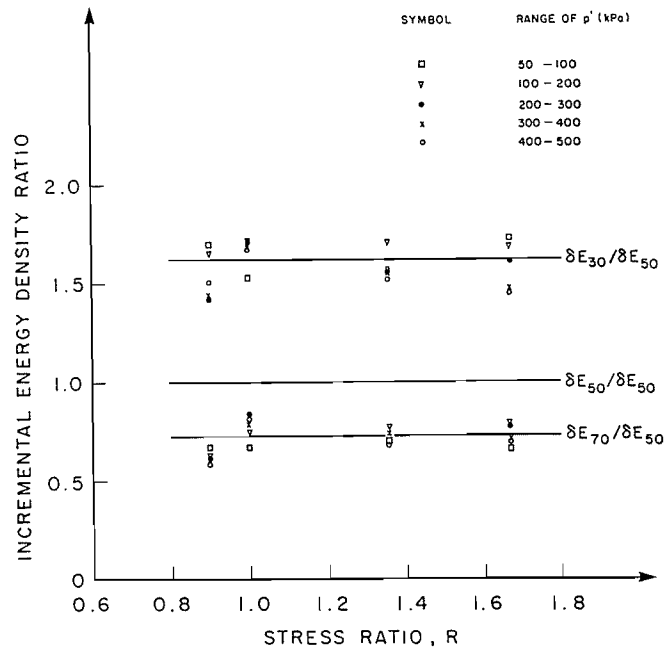

FIG. 12. Relationships between incremental energy density ratio with stress ratio.

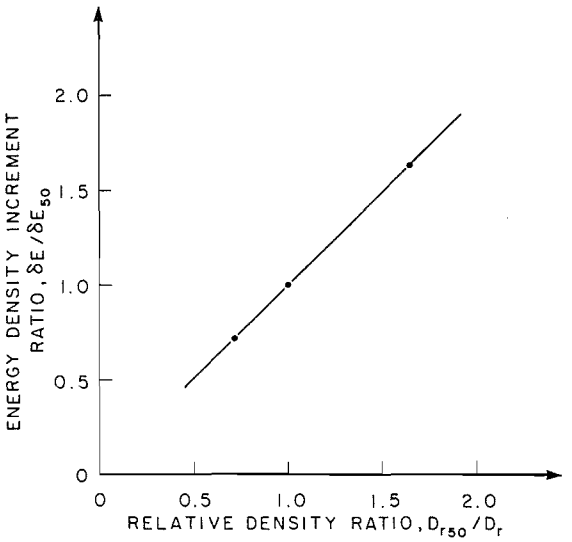

FIG. 13. Relationships between ratios of energy density increment and relative density.

relative densities in Fig. 13. A linear relationship with a slope equal to unity is obtained. Thus

$$[11] \quad \frac{\delta E_1}{\delta E_2} = \frac{D_{r2}}{D_{r1}}$$

in which the subscripts on E and D_r associate corresponding energy and relative density states D_{r1} and D_{r2}. Equation [11] may be stated as follows:

Given two specimens at relative densities D_{r1} and D_{r2} proportionally loaded under identical R to mean effective stress p', if identical stress increments $\delta p'$ were to be applied to each specimen, energy density increments of δE_1 and δE_2 would take place. The ratio of these energy density increments is equal to the inverse ratio of their relative densities, regardless of the indentical R value under which proportional loading occurred. Using [8], the energy density increment ratio may be written in terms of strain increments as

$$[12] \quad \frac{\delta E_1}{\delta E_2} = \frac{\delta\epsilon_{a1}\left(R + \dfrac{\sqrt{2}}{\tan\theta_1}\right)}{\delta\epsilon_{a2}\left(R + \dfrac{\sqrt{2}}{\tan\theta_2}\right)}$$

and from [11],

$$[13] \quad \frac{D_{r2}}{D_{r1}} = \frac{\delta\epsilon_{a1}\left(R + \dfrac{\sqrt{2}}{\tan\theta_1}\right)}{\delta\epsilon_{a2}\left(R + \dfrac{\sqrt{2}}{\tan\theta_2}\right)}$$

in which $(\delta\epsilon_{a1}, \theta_1)$ and $(\delta\epsilon_{a2}, \theta_2)$ are associated with relative densities D_{r1} and D_{r2} respectively and the stress ratio R.

Proportional loading stress–strain relationship

Equation [13] enables prediction of axial strain increments at any desired relative density from a known stress–strain relationship at another relative density, provided the stress histories (p', R) of two samples are identical. Earlier, [3] was shown to enable predictions of axial strain increments under any stress ratio from a known stress–strain relationship at another stress ratio, provided the two samples have identical relative densities. It is thus possible to predict axial strain increments under any relative density D_r and stress ratio R by a simple superposition of an identical relative density process ([3]) and an identical stress history process ([13]).

Considering the identical relative density process ([13]), the axial strain increment $\delta\epsilon_a'$ under R at D_{ri} is given by

$$[14] \quad \delta\epsilon_a' = \frac{\sin\theta'}{\sin\theta_i}\frac{\cos(\theta_i - \psi)}{\cos(\theta' - \psi)}\delta\epsilon_{a_i}$$

in which $\delta\epsilon_{a_i}$ is the known axial strain increment at D_{ri} and R_i, and θ_i and θ' are associated with strain increment ratios at relative density D_{ri} under R_i and R respectively. Both θ_i and θ' can be evaluated for their respective stress ratio and relative densities from [9] or [10]. Now following next a constant stress history process ([13]), the desired axial strain increments at D_r and R are related to $\delta\epsilon_a'$ by

$$[15] \quad \delta\epsilon_a = \frac{D_{ri}}{D_r}\frac{R + \dfrac{\sqrt{2}}{\tan\theta'}}{R + \dfrac{\sqrt{2}}{\tan\theta}}\delta\epsilon_a'$$

in which θ is associated with strain increment ratio at D_r under R. Substituting for $\delta\epsilon_a'$ from [14] into [15], we get

$$[16] \quad \delta\epsilon_a = \left[\frac{D_{ri}}{D_r}\right]\left[\frac{\left(R + \dfrac{\sqrt{2}}{\tan\theta'}\right)}{\left(R + \dfrac{\sqrt{2}}{\tan\theta}\right)}\right]\left[\frac{\sin\theta'}{\sin\theta_i}\frac{\cos(\theta_i - \psi)}{\cos(\theta' - \psi)}\right]\delta\epsilon_{a_i}$$

Since strain increment ratio $\delta\epsilon_a/\delta\epsilon_r$ $(=\sqrt{2}\tan\theta)$ is uniquely prescribed by the plane surface in [9] and [10], once R and D_r are specified, the radial strain increment $\delta\epsilon_r$ (or volumetric strain increment $\delta\epsilon_v$) can be readily calculated. Hence a complete stress–strain response under any R at D_r can be predicted from a known response under a known R_i and D_{ri}. In [16] the three terms in the square brackets may be considered to reflect respectively the influences of (1) relative density, (2) variation in anisotropy due to changes in relative density, and (3) the effect of stress path.

Equation [16] has been used to develop stress–strain predictions for specimens at 30, 50 and 70% relative densities (Figs. 14–16). Predictions are made for proportional loading under hydrostatic as well as in compressional and extensional modes and are compared with the measured response. The known data base for these predictions consists of hydrostatic loading (R = 1) at a relative density of 50%. It may be seen that excellent agreement exists between predicted and observed response in each case. The agreement between predicted and measured axial strain response for loose sand in extensional loading (Fig. 15*a*) may appear unsatisfactory. However, considering the extremely small magnitude of strains, the agreement can be regarded as rather good.

It may be pointed out that the proposed stress–strain relationship does not require any appeal to material isotropy, which is generally needed in most stress–strain formulations. The effect of inherent anisotropy in sand, which is considered to be associated with the one-dimensional sedimentation process, is inherently built into the proposed relationships. Furthermore, unlike most other stress–strain relationships, the proposed

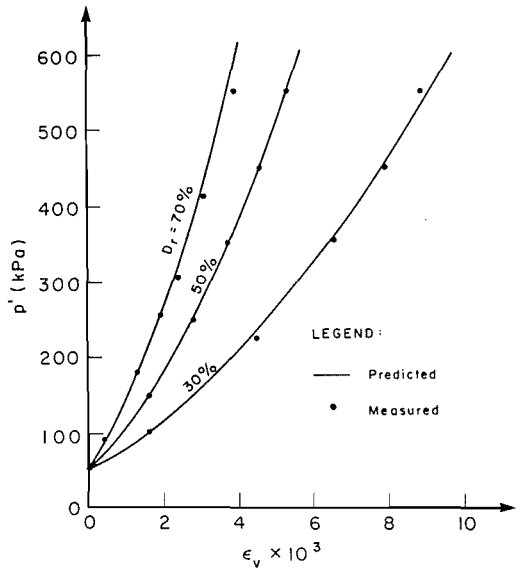

FIG. 14. Comparison of measured and predicted volumetric strains for hydrostatic loading.

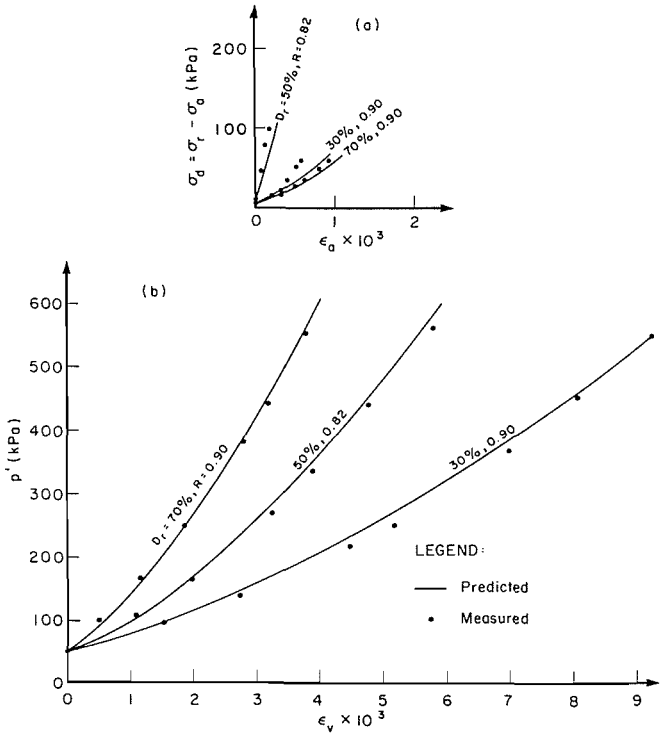

FIG. 15. Comparison of measured and predicted strains: (*a*) axial strain; (*b*) volumetric strain.

relationship takes account of relative density in the form of an independent-state variable, enabling stress–strain predictions from one relative density state to another. In other words, hydrostatic and anisotropic consolidation states (which represent states arrived at through proportional loading) at different relative densities can be quantitatively related.

Required parameters

In all, four parameters, A, B, C (or D), and angle ψ, are required for the complete stress–strain relationship. Constants A, B, and C (or D) determine the unique plane surface from

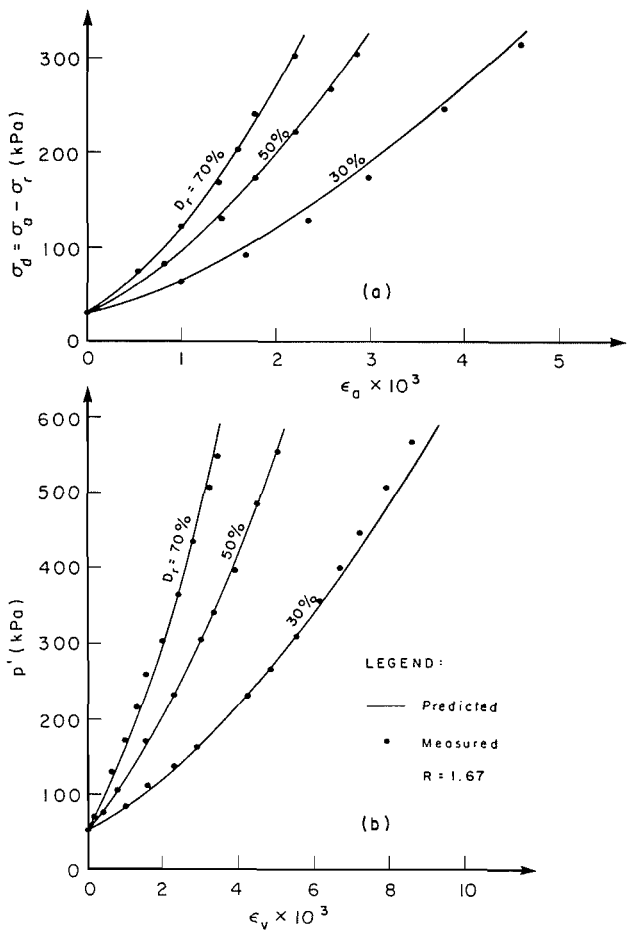

FIG. 16. Comparison of measured and predicted strains: (*a*) axial strain; (*b*) volumetric strain.

which strain increment ratio (or θ) for any desired R and D_r can be determined. In adition, angle ψ is needed for evaluating axial strain increments for the desired R and D_r ([16]). All four constants can be determined from three triaxial tests. Two of these constant R tests must be at the same relative density in order to determine parameter ψ. The third test must be at another value of relative density. For simplicity, two tests at different relative densities can be the conventional hydrostatic compression tests ($R = 1$). The three tests together thus provide the required three points in R, D_r, and θ space for defining the equation of the plane surface ([9] or [10]). The results of any one of the three tests can be used as the reference data base for prediction of stress–strain behaviour under arbitrary R path and desired D_r.

Conclusions

Constant stress ratio (proportional loading) response of sand, for which all strain components are entirely compressive, has been studied under stress conditions of the triaxial test. Linear strain paths were observed to result from proportional loading. Effective mean normal stress equipotentials were found linear and parallel in strain space. The gradient of these equipotentials, ψ, was found to be constant and independent of relative density.

Tangent inverse of strain increment ratio was found to be linearly related to stress ratio at each relative density. This characteristic, together with the constant value of ψ, enabled formulation of a proportional loading stress–strain relationship for the sand at one relative density. It was also found that the

energy density increment ratio of two R paths at the same relative density remains constant.

Identical stress histories were found producing an energy density increment ratio that is equal to the inverse ratio of the respective relative densities. Relationships between stress ratio and strain increment ratio and relative density were found to describe a unique plane in three-dimensional space. These two characteristics were used to formulate a complete proportional loading stress–strain relationship to predict strain increments along any desired R path and relative density. Only three constant R tests are required to obtain the necessary parameters for the stress–strain relationship.

Acknowledgements

Financial assistance of the Natural Sciences and Engineering Research Council of Canada is gratefully acknowledged. Richard Brun drafted the figures and Mrs. Kelly Lamb typed the manuscript. The machining skills of Fred Zurkirchen and various discussions wih him were very helpful. Constructive comments and valuable suggestions for improvement of the paper were made by the reviewers. The authors acknowledge their assistance with deep appreciation.

ARTHUR, J. R. F., and MENZIES, B. K. 1972. Inherent anisotropy in sand. Géotechnique, **22**(1), pp. 115–128.

BARDEN, L., KHAYATT, A. J., and WIGHTMAN, A. 1969. Elastic and slip components of the deformation of sand. Canadian Geotechnical Journal, **6**(3), pp. 227–240.

COON, M. D., and EVANS, R. J. 1969. Discussion on 'Elastic behaviour of cohesionless soils' by I. Holubec. ASCE Journal of the Soil Mechanics and Foundations Division, **95**(SM5), pp. 1281–1283.

DUNCAN, J. M., and CHANG, C. Y. 1970. Nonlinear analysis of stress and strain in soils. ASCE Journal of the Soil Mechanics and Foundations Division, **96**(SM5), 1629–1653.

EL-SOHBY, M. A. 1969. Deformation of sands under constant stress ratios. Proceedings, 7th International Conference on Soil Mechanics and Foundation Engineering, Mexico, Vol. 1, pp. 111–119.

EL-SOHBY, M. A., and ANDRAWES, K. Z. 1972. Deformation characteristics of granular materials under hydrostatic compression. Canadian Geotechnical Journal, **9**(4), pp. 338–350.

GREEN, G. E. 1969. Strength and compressibility of granular materials under generalized strain conditions. Ph.D. thesis, University of London, London, England.

MEHAN, R. L. 1961. Effect of combined stress on yield and fracture behaviour of zircaloy-2. Journal of Basic Engineering, **83**, pp. 499–512.

NEGUSSEY, D. 1984. An experimental study of the small strain response of sand. Ph.D. thesis, University of British Columbia, Vancouver, B.C.

ODA, M. 1972. Initial fabrics and their relations to mechanical properties of granular material. Soils and Foundations, **12**(1), pp. 17–36.

POOROOSHASB, H. B., HOLUBEC, I., and SHERBOURNE, A. N. 1966. Yielding and flow of sand in triaxial compression, Part I. Canadian Geotechnical Journal, **3**(4), pp. 179–190.

REES, D. W. A. 1981. A hardening model for anisotropic materials. Experimental Mechanics, **21**, pp. 245–254.

ROWE, P. W. 1962. The stress-dilatancy relation for static equilibrium of an assembly of particles in contact. Proceedings of the Royal Society of London, Series A, **269**, pp. 500–527.

ROWE, P. W. 1971. Theoretical meaning and observed values of deformation parameters for soil. Proceedings of the Roscoe Memorial Symposium on Stress–Strain Behaviour of Soils, Cambridge University, pp. 143–196.

ROWE, P. W., and BARDEN, L. 1964. The importance of free ends in the triaxial test. ASCE Journal of the Soil Mechanics and Foundations Division, **90**(SM1), Proceedings Paper 3753, pp. 1–27.

SARSBY, R. W., KALTEZIOTIS, N., and HADDAD, E. H. 1980. Bedding error in triaxial tests on granular media. Géotechnique, **30**(3), pp. 302–309.

VAID, Y. P., and NEGUSSEY, D. 1983. A simple stress path analog for the triaxial test. Canadian Geotechnical Journal, **20**(4), pp. 827–832.

——— 1984. A critical assessment of membrane penetration in the triaxial test. Geotechnical Testing Journal, **7**, pp. 70–76.

YAMADA, Y., and ISHIHARA, K. 1979. Anisotropic deformation characteristics of sand under three dimensional stress conditions. Soils and Foundations, **19**(2), pp. 79–94.

ZYTYNSKI, M., RANDOLPH, M. F., NOVA, R., and WROTH, C. P. 1978. On modelling the unloading–reloading behaviour of soils. International Journal for Numerical and Analytical Methods in Geomechanics, **2**, pp. 87–94.